Langmuir

Article

pubs.acs.org/Langmuir

Self-Seeded Growth of Five-Fold Twinned Copper Nanowires: Mechanistic Study, Characterization, and SERS Applications

Hong-Jie Yang, Sheng-Yan He, and Hsing-Yu Tuan*

Department of Chemical Engineering, National Tsing Hua University, 101, Section 2, Kuang-Fu Road, Hsinchu, Taiwan 30013, Republic of China

Supporting Information

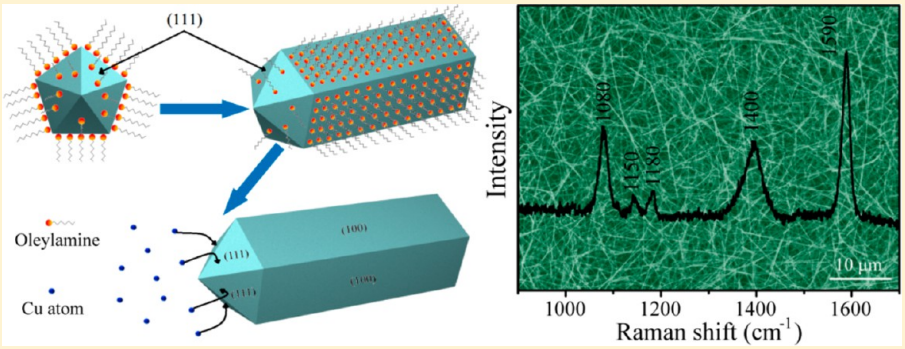

ABSTRACT: A comprehensive mechanistic study conducted on the formation mechanism of five-fold twinned copper nanowires by heating copper(I) chloride with oleylamine at 170 °C is presented. Electron microscopy and UV−visible absorption spectra are used to analyze the growth mechanism of copper nanowires. High-resolution transmission electron microscopy and selected-area electron diffraction are used to investigate the detailed structure of copper nanowires and nanoparticles, and a five-twinned structure is shown to exist in the copper nanowires and nanoparticles. Additionally, experiments have been performed to indirectly confirm that oleylamine preferentially adsorbs on the {100} facets of growing crystals. On the basis of the above results, the self-seeded growth of copper nanowires is confirmed. In the initial stage of reactions, copper nanoparticles with two distinctive sizes are formed. As the reaction proceeds, larger five-twinned copper nanoparticles serve as seeds for anisotropic crystal growth. Further, copper atoms generated from an Ostwald ripening process or reduction reactions of a copper(I) chloride−oleylamine complex continue to deposit and crystallize on the twin boundaries. Once the {110} planes are generated, oleylamine preferentially adsorbs on the newly formed {100} facets and then guides the formation of nanowires. The electrical resistivity of a single copper nanowire is measured to be 41.25 nΩ-m, which is of the same order of magnitude as the value of bulk copper (16.78 nΩ-m). Finally, an effective surface-enhanced Raman spectroscopy active substrate made of copper nanowire is used to detect the 4-mercaptobenzoic acid molecules.

INTRODUCTION

Copper (Cu) is one of the most important industrial metals in modern technologies, which has been used as an interconnection in a wide variety of commercial applications,[1] especially in the form of wires, owing to its high electrical and thermal conductivity and lower cost. However, with the shrinking size of commercial integrated circuits, the size of Cu wires must be correspondingly reduced. At the nanoscale, the chemical, electrical, mechanical, and optical properties of Cu nanowires would be altered.[2,3] Cu nanowires have attracted considerable attention in recent years because of their potential applications for broader fields, such as nanoprobes, optical devices, and a low-cost alternative to indium tin oxide for use as a transparent electrode.[4−10] Among the various synthetic routes, solution-phase synthesis is the most extensively used because of its simplicity, low cost, and ease of scalability.[11−15] For example, Liu et al. synthesized Cu nanowires in large quantities by reducing Cu−glycerol complexes using phosphite in the presence of sodium dodecyl benzenesulfonate using a hydrothermal process.[16] Chang and co-workers developed a facile aqueous reduction route to produce high-quality ultralong Cu nanowires through the reduction of copper(II) nitrate.[17] Cu nanowires were also produced using other synthetic approaches.[16−21]

Seed-mediated growth is the most successful method of producing one-dimensional (1-D) metal nanostructures. For a metal with a highly symmetric face-centered cubic structure, such as Cu, silver (Ag), and gold (Au), an external force is needed to promote anisotropic growth for the formation of metal nanowires. Metal nanowires synthesized using a seed-mediated growth approach or a self-seeded process usually possess a pentagonal cross section along the nanowire

Received: September 18, 2013
Revised: December 22, 2013
Published: December 24, 2013

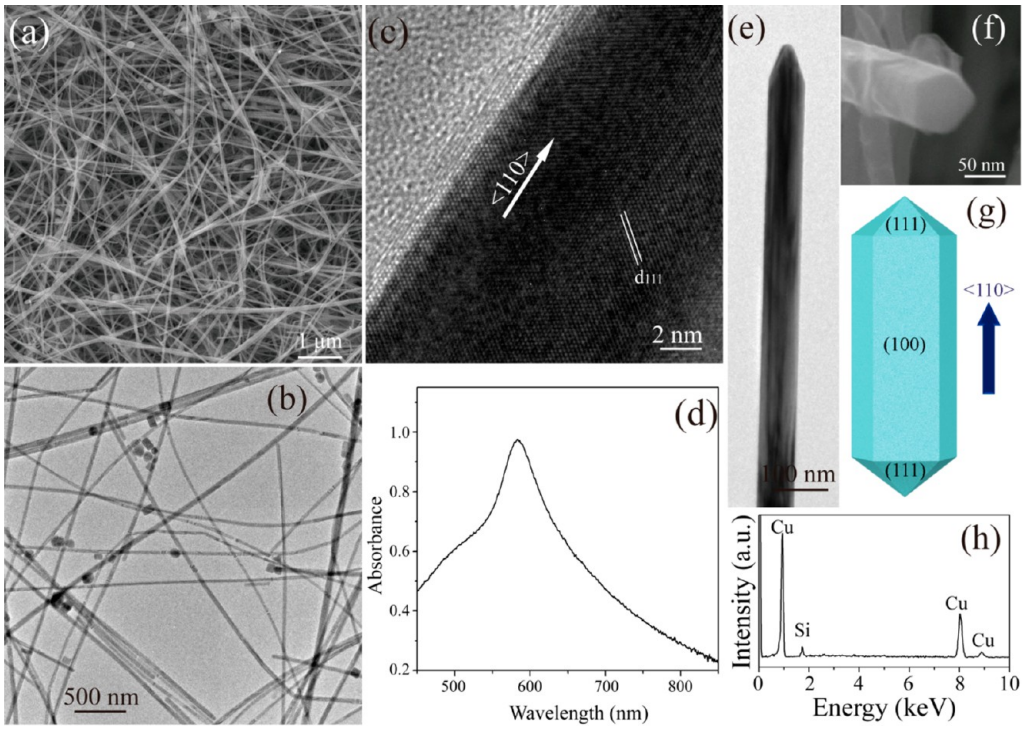

Figure 1. Cu nanowires synthesized by heating CuCl with OLA at 170 °C for 61 h. (a) SEM image and (b) TEM image show that the product is mainly composed of Cu nanowires. (c) HRTEM image of Cu nanowire growth along ⟨110⟩ direction. (d) UV−visible spectra of the Cu nanowires. (e) TEM image of one end of nanowire and (f) cross-sectional SEM image that confirms that the nanowire has a pentagonal cross section. (g) Schematic model of the nanowires. (h) EDS spectra of the Cu nanowires reveals Cu and Si elements.

body.[22−28] The seed-mediated method involves introducing twin defects in the seed crystals as the inner confinement and the capping agent as the outer confinement to the synthetic environment to promote metal nanowire formation. Five-twinned seeds with a decahedral profile surrounded by a mix of {111} and {100} facets that serves as the inner confinement prefer to grow along the parallel axis to avoid any increase in the lattice strain energy.[29,30] Some of the 1-D metal structures have been observed in the gas phase without the use of capping reagent, which could indicate that the twin defects induce 1-D growth.[31−33] In addition, capping agents are known to play an important role in the synthesis of 1-D nanomaterials by preferential adsorption on the specific surface in solution phase, which serves as the outer confinement.[34] For example, poly(vinylpyrrolidone) (PVP) is used as a typical capping agent in polyol reactions and plays an important role in producing Ag nanowire having a pentagonal cross section through preferential adsorption on the {100} facets of five-twinned Ag seeds.[35] Several studies have been reported on the growth mechanism and detailed structural analysis of metal nanorods or nanowires derived from five-twinned particle seeds.[36−38] However, these studies mainly focused on 1-D Ag or Au nanomaterials. To date, a mechanistic study on the formation of 1-D Cu nanostructures with a five-fold twinned structure is not available.

In this paper, we present a comprehensive mechanistic study on the reaction of copper chloride with oleylamine (OLA) that produces Cu nanowires having five-fold twinned structure which has rarely been studied in the past. An electron microscope and a UV−visible absorption spectrometer were used ex situ to monitor the morphological evolution of the Cu nanocrystals during the course of the reactions. The detailed microstructures of the five-twinned seeds and pentagonal Cu nanowires have also been studied using high-resolution transmission electron microscopy (HRTEM). It is proposed that OLA assists the growth of nanowires and preferentially adsorbs on the {100} facets based on the results of experiments performed. From the obtained results, the self-seeded process was confirmed as the growth mechanism of the Cu nanowires, where five-twinned seeds were produced in situ and then nanowires were formed with the assistance from OLA by effectively stabilizing the newly formed {100} facets. A single Cu nanowire has a low electrical resistivity of 41.25 nΩ-m measured using a four-probe technique. Finally, the efficiency of Cu nanowires employed as a surface-enhanced Raman spectroscopy (SERS)-active substrate for detecting the 4-mercaptobenzoic acid molecules is demonstrated for the first time.

EXPERIMENTAL SECTION

Chemicals. Copper(I) chloride (CuCl, 99.995%), oleylamine (OLA, 70%), 1-octadecene (ODE, 90%), ethanol (>99.8%), toluene (>99.9%), hydrogen peroxide (30 wt % in H_2O), sulfuric acid (95−98%), and 4-mercaptobenzoic acid (4-MBA, 99%) were obtained from Sigma-Aldrich, stored in a glovebox to prevent oxygen and moisture, and used without further purification.

Synthesis of Cu Nanowires. The CuCl−OLA mixture solution was prepared by mixing 25 mg of CuCl with 5 mL of OLA in a 20 mL glass vial. The solution mixture was then heated up to 170 °C using an oil bath while stirring. The solution turned to pale yellow at about 100 °C. As the reaction progressed, the color of the solution gradually changed to reddish brown, indicating a Cu precipitate. The reaction was allowed to proceed at 170 °C for 61 h. The Cu nanowires were washed by adding 30 mL of toluene in the reaction mixture with sonication for 10 s followed by centrifugation at 8000 rpm for 5 min and repeated several times. The precipitated Cu nanowires were stored in the glovebox for further characterization.

dx.doi.org/10.1021/la4036198 | Langmuir 2014, 30, 602−610

Characterization. The morphologies of the products were examined with scanning electron microscopy (SEM, Hitachi S-2300) and transmission electron microscopy (TEM, JEOL, JEM 2100F and FEI-TEM, Philips Tecnai G2 operating at 200 kV). Additionally, the HRTEM images and selected-area electron diffraction (SAED) patterns were obtained on an FEI-TEM (Philips Tecnai G2 operating at an accelerating voltage of 200 kV). The elemental composition of the Cu nanowires was obtained by energy dispersive X-ray spectroscopy (EDS). Moreover, X-ray diffraction (XRD) patterns were recorded with an X-ray diffractometer (Rigaku Ultima IV) using Cu Kα radiation (λ = 1.54178 Å) operated at a scanning rate of 1°/min. Thereafter, UV−visible absorption spectra of Cu nanowire solutions (the reaction mixtures were diluted with toluene) were obtained with a Hitachi U-4100 spectrophotometer using a quartz cuvette having a 1 cm optical path. The electrical transport properties of the Cu nanowires were observed with a home-built probe station equipped with a Keithley 236 semiconductor parameter analyzer. Subsequently, some of these nanowires were transferred onto Si chips with photolithographically prepatterned Au/Ti microelectrodes. A focused ion beam (FIB, FEI Nova 200) system was used to connect four gold electrodes and a Cu nanowire with thin platinum leads. Raman (SERS) spectra of samples were recorded with a Jobin-Yvon HR800 Raman system using a 632.8 nm He:Ne laser line for excitation with a spot size of 1 μm in diameter and a power of 10 mW with a 3 cm^{-1} resolution. The integration time was 10 s for each spectrum. For preparation of SERS substrates, the silicon substrate (1 cm × 1 cm) was first immersed into the piranha solution (hydrogen peroxide/sulfuric acid at a volumetric ratio of 1:3) for 10 min at 90 °C, washed with ethanol and water sequentially, and then blow dried with nitrogen gas. For preparation of Cu nanowires substrates, 0.5 mL of Cu nanowires dispersed in toluene (1 mg/mL) were sonicated for 10 min and then dropped on a silicon substrate (1 × 1 cm^2). The SERS samples were prepared by immersing Cu nanowire substrates in 4 mL of 2.5 mM 4-MBA in ethanol solution for the desired time. Then it was rinsed with ethanol and dried in air.

RESULTS AND DISCUSSION

It is well-known that OLA can coordinate to metal ions to form metastable compounds.[39] In our approach, a Cu^+−OLA complex forms when a CuCl−OLA solution is heated to about 100 °C; Cu atoms can be simply generated by elevating the temperature of the metastable compound solution. Figure 1 shows the morphology and dimensions of the nanowire products obtained by heating CuCl with OLA at 170 °C for 61 h. Figure 1a shows the typical SEM image of Cu nanowires and illustrates that the reaction product is mainly composed of a large quantity of nanowires. The prepared nanowires are primarily straight with a mean diameter of 63 nm, with the diameter mostly distributed between 50 and 80 nm. The cross-sectional SEM images, shown in Figure 1f, confirm that the nanowires possess pentagonal cross sections, indicating the five-twinned structure of the Cu nanowires. Figure 1g shows a schematic model of the nanowires, and Figure 1b shows the TEM image of the Cu nanowires randomly arranged on the TEM grid, which further confirms the morphology of the nanowires. The structure of these Cu nanowires was further investigated with a HRTEM. Figure 1c shows the HRTEM image of an individual Cu nanowire with well-resolved (111) lattice fringes having a spacing of 0.21 nm, which confirms that the growth of the nanowire is along the ⟨110⟩ direction. A typical image of the EDS spectrum (Figure 1h) shows that the nanowires are composed of Cu and silicon (Si) elements. The presence of the Cu signal in the EDS spectrum confirms the formation of Cu nanowires, whereas the Si signal originates from the Si substrate. Figure 1d shows the UV−visible absorption spectrum of the Cu nanowire solution. The Cu nanowires exhibit a major LSPR peak at 583 nm. The XRD pattern (Figure 2) suggests that the Cu nanowires have a face-centered cubic structure (JCPDS file no. 03-1018). Further, no characteristic peaks of impurities (CuO or Cu_2O) were detected, indicating pure Cu nanowires.

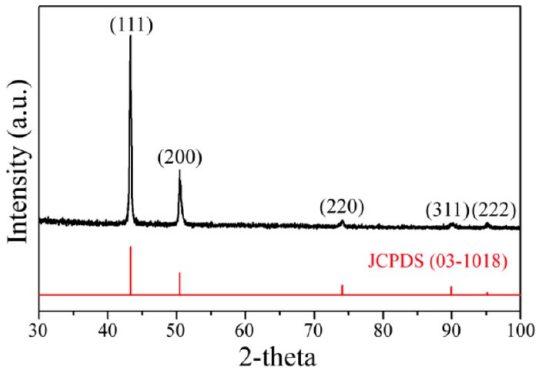

Figure 2. XRD pattern of the Cu nanowires.

To investigate the growth process and explain the possible growth mechanism of Cu nanowires, the samples were systematically analyzed at different time intervals using TEM and SEM. Although the reactions proceeded faster at higher temperatures, to better capture the morphology transformation of Cu nanocrystals and explain the growth process of Cu nanowires, we chose a relatively low temperature (170 °C) to carry out the reaction and make the overall reaction time longer. Figure 3 shows the electron microscopy (TEM and SEM) images of the products that were obtained at 170 °C after the reaction proceeded for 8, 12, 16, 19, 48, and 61 h, respectively. These images clearly show the morphological evolution of the Cu nanostructures from nanoparticles to nanowires over the 61 h reaction time at 170 °C. After 8 h, the color of the CuCl−OLA solution changed from pale yellow to pale red, indicating the formation of Cu nanoparticles through the slow reduction of CuCl by OLA.[19,20] Figure 3a shows the TEM image of the initial product, after 8 h of reaction time, consisting of nanoparticles having two distinctive sizes via homogeneous nucleation processes. The majority of these nanoparticles had sizes <10 nm, and the others were larger nanoparticles (20−40 nm in diameter). Further, the surface energies of the larger particles are lesser than those of smaller ones. Therefore, when the reaction was carried out continuously at 170 °C, the small Cu nanoparticles gradually dissolved in the solution to generate Cu atoms and recrystallized on the larger ones via a well-known process: the Ostwald ripening mechanism. After 12 h of reaction time, the number of smaller nanoparticles decreased, and the larger nanoparticles continued to grow with diameters ranging from 40 to 70 nm. Moreover, a few short nanorods began to appear, as shown in Figure 3b. In our system, we believe that OLA plays three roles: solvent, reducing agent, and capping agent. With the assistance of OLA, some of the larger Cu nanoparticles grow into the rod-shaped structure. The role of OLA in the formation of Cu nanowires is similar to that of PVP in the formation of Ag nanowires.[22] As the reaction time continues to increase to 16, 19, 48, and 61 h (Figure 3c−f), the reaction system goes into a transitional period from nanoparticles to nanowires. As the reaction time increases, the number of nanoparticles decrease, whereas the number of nanowires increase. In addition, the length of the Cu nanowire also increases significantly because

dx.doi.org/10.1021/la4036198 | Langmuir 2014, 30, 602−610

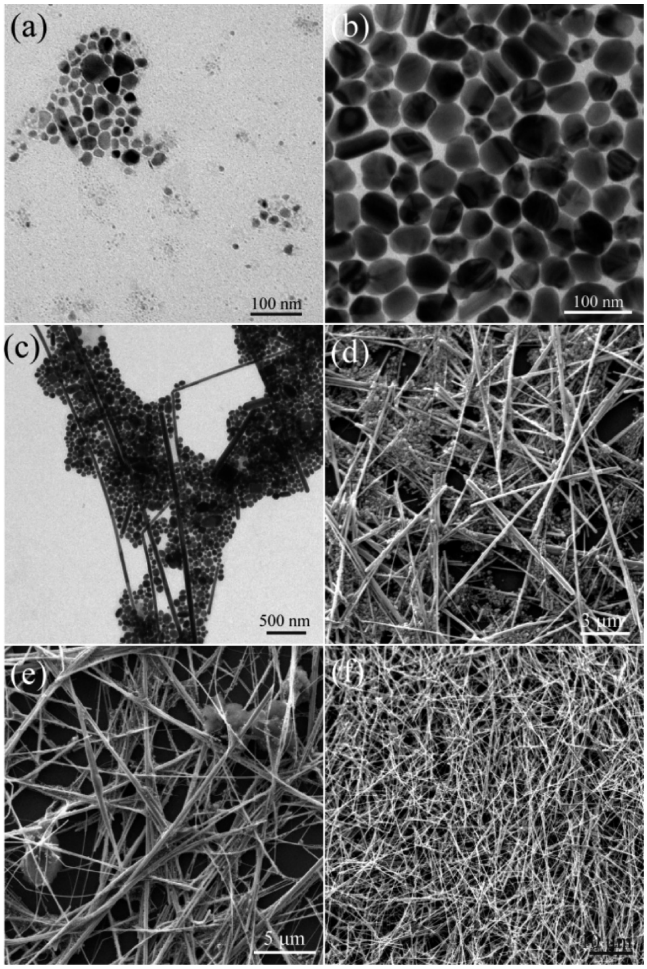

Figure 3. (a, b, c) TEM and (d, e, f) SEM images of six different products recorded at (a) 8, (b) 12, (c) 16, (d) 19, (e) 48, and (f) 61 h of reaction time, respectively, showing the morphological evolution of Cu nanostructures.

the lateral facets, {100} planes, were passivated by OLA. In a typical synthesis, the nanowires obtained at 19 h are short, with lengths less than 10 μm (Figure 3d); however, they grow to 30 μm after the reaction proceeds for 61 h (Figure 3f).

The UV−visible spectroscopy procedure has been conducted to track the morphological evolution involved in the growth process because the surface plasmon resonance bands of metal nanostructures are affected by their shape.[40−42] Figure 4 illustrates a comparison of the variation of the UV−visible absorption spectra obtained from the solutions at different reaction times from 8 to 61 h. At 8 h, the appearance of a broad plasma peak at approximately 630 nm, indicating the existence of a broad distribution in size, can be attributed to the formation of Cu nanoparticles. As the reaction proceeds for approximately 12 h, the peak position further blue shifts from 630 to 615 nm, which implies the formation of short Cu nanorods. Between 16 and 48 h, the intensity of plasma peak at 580−590 nm further increases rapidly and gradually becomes sharp, indicating that the amount and length of the nanowires increases and the number of Cu nanoparticles decreases. Finally, the plasma peak of the Cu nanowires slightly red shifts from 581 to 583 nm, indicating an increase in size of the Cu nanowires as the reaction time proceeds from 48 to 61 h.

To verify that the five-twinned structure exists in the Cu nanocrystals and nanowires, HRTEM was performed to study

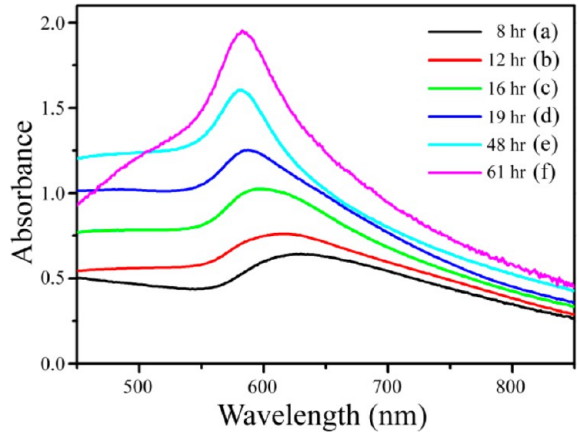

Figure 4. UV−visible spectra of the reaction mixture at different reaction times: (a) 8, (b) 12, (c) 16, (d) 19, (e) 48, and (f) 61 h.

the detailed structure of the Cu nanostructures. Figure 5a and 5c shows the HRTEM images of the Cu nanoparticles

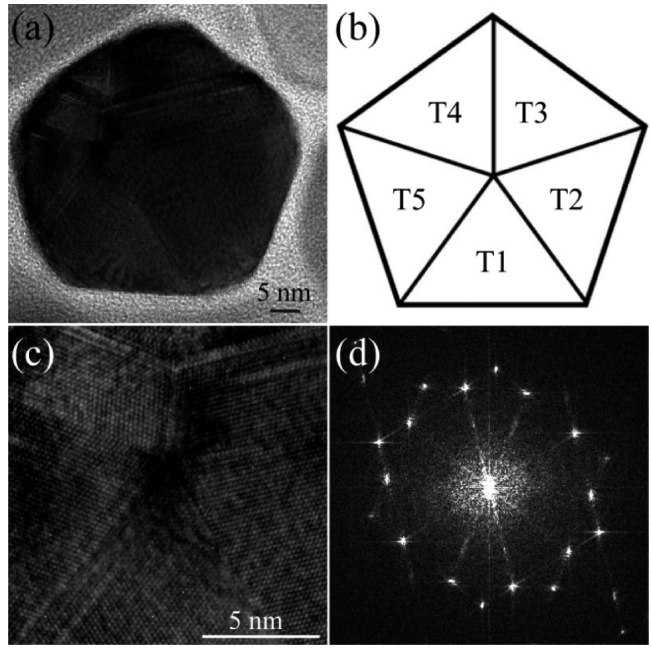

Figure 5. (a) HRTEM images of a Cu nanoparticle generated at 12 h. (b) Schematic diagram of a Cu nanoparticle composed of five face-centered cubic Cu subcrystals. (c) Higher magnification HRTEM image of the Cu nanoparticle in panel a. (d) Fast Fourier transform of the nanoparticle shown in panel c.

generated after 12 h of reaction time. The Cu particles have a diameter of approximately 50 nm with five distinctive boundaries. The clear lattice image indicates that the Cu nanoparticles are five-twinned crystals with some stacking faults. The fast Fourier transform (FFT) of the Cu nanoparticle shown in Figure 5d demonstrates a typical five-fold symmetry and can be well interpreted by superimposing five face-centered cubic Cu subcrystals (Figure 5b, T1 to T5) with a [110] orientation, indicating that the nanoparticles have five-twinned structure. A five-fold twinned nanorod bounded by five {100} planes and capped by ten {111} planes was used to represent the structure of Cu nanowires. The nanorods consist of five identical subunits labeled as T1−T5, as shown in Figure 6a and

dx.doi.org/10.1021/la4036198 | *Langmuir* 2014, 30, 602−610

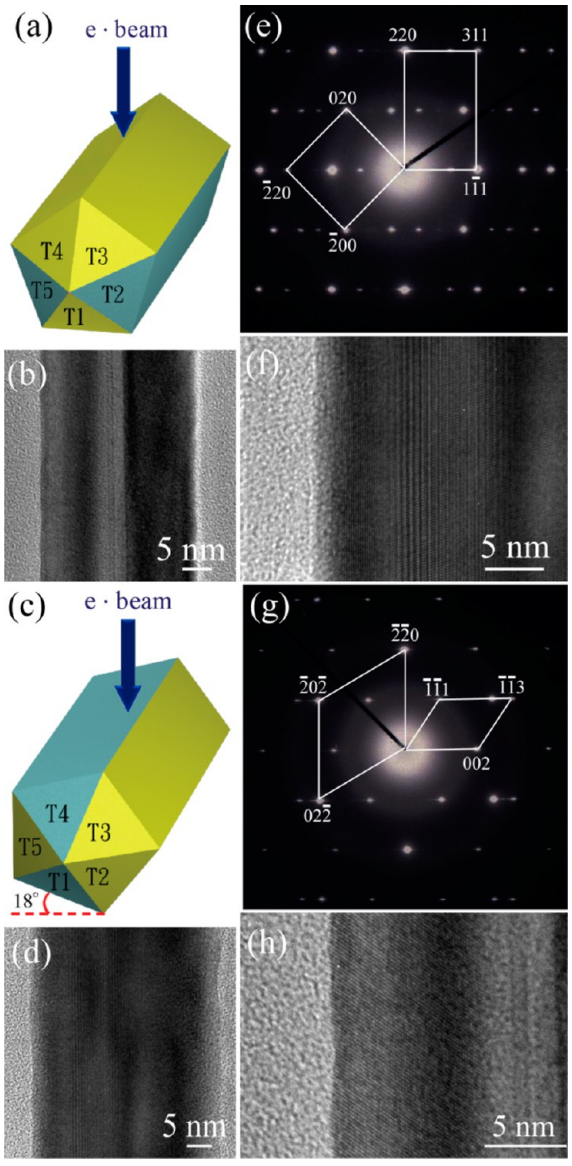

Figure 6. Structural model of the five-fold twinned nanowire consists of five identical subunits labeled T1−T5, and the electron beam runs perpendicular (a) and parallel (c) to one side surface of the nanowire. (b) TEM, (e) SAED pattern, and (f) HRTEM image when the electron beam runs perpendicular to one side surface of the nanowire. (d) TEM, (g) SAED pattern, and (h) HRTEM image when the electron beam runs parallel to one side surface of the nanowire.

6c.[37,43] Figure 6b,d,e−h shows the HRTEM and SAED patterns of the Cu nanowire obtained when the electron beam runs perpendicular (Figure 6a) and parallel (Figure 6c) to one side surface of the nanowire. When the electron beam is perpendicular to one side surface of the nanowire, the SAED pattern is found to be a superimposition of two face-centered cubic patterns composed of zone [001] generated from T1 and zone [112] generated from T3 and T4, indicating that the Cu nanowire is not a single crystal. The remaining reflection spots in Figure 6e can be interpreted by the double-diffraction effects through the subcrystals and the twin boundary-related diffraction.[44] The TEM and HRTEM images (Figure 6b and 6f) clearly show that the [111] twin plane is oriented parallel to its longitudinal axis. If the electron beam runs parallel to one side surface of the nanowire, the SAED pattern will be composed of the [110] zone axis direction generated from T5 and the [111] direction generated from T2 and T3, as shown in Figure 6g. The TEM and HRTEM images of a Cu nanowire in Figure 6d and 6h also reveal a twin structure. These observations suggest that the Cu nanowires should possess a multiple-twinned structure, which is consistent with the results obtained for the metal nanorods or nanowires having pentagonal cross sections.[37,45−47]

From the electron microscope and UV−visible data, Cu nanowires grown from multiple-twinned seeds and having pentagonal cross sections are shown to have a five-twinned structure bounded by five {100} planes and capped by ten {111} planes. Initially, the five-twinned seeds are formed by homogeneous nucleation. As the reaction proceeds, the Ostwald ripening process consumes smaller nanoparticles to offer Cu atoms and recrystallize them on the relatively larger five-twinned seeds. The nanoparticles with five-twinned structures serve as internal confinement because the twin boundary has the highest energy site on the surface, leading to continuous twin growth on it.[48] Moreover, the five-twinned seeds also prefer to grow along the parallel axis to avoid any increase in strain energy and then generate the new {110} planes, so they can prevent the formation of larger nanoparticles instead of nanorods. Here, OLA is a capping ligand that serves as an outer confinement. After the {110} planes are generated, the OLA adsorbs and binds preferentially on the newly formed {100} facets because the {100} planes offer more open sites to interact with OLA and inhibit the radial growth rate.[43] As a result, nanorods continuously elongate into nanowires having pentagonal cross sections. In addition, so far there is no generally accepted theoretical model or measurement method for determining the interaction strengths of surfactant with specific facets on a nanocrystal surface.[49,50] We therefore performed a few tests to indirectly prove that OLA preferentially adsorbed on the {100} facets and guided the formation of nanowires. First, we conducted a series of experiments with different amounts of OLA (other reaction parameters remain unchanged) to understand its effect on the morphology of products. To maintain the reaction volume constant, we chose a noncoordinating solvent, ODE, which does not act as a surfactant and has low reactivity with CuCl. When the reaction solvent was replaced by ODE, the CuCl did not react with ODE to form a complex, and the reaction mixture remain unchanged after 61 h (Figure 7a). Figure 7b−d shows the SEM images of Cu nanostructures generated at different amounts of OLA. When only 0.12 mL of OLA was used in the reaction (Figure 7b), most products were nanoparticles, and nanowires appeared with larger diameter (>200 nm) and shorter length (<2 μm). When the amount of OLA respectively increased to 0.36 mL (Figure 7c) and 1 mL (Figure 7d), the proportion and the length of nanowires in the products significantly increased. Second, we performed reactions in the presence of preformed Cu seeds taken from typical reactions at 170 °C for 12 h, and the other reaction conditions remained unchanged. We can easily observe the formation of Cu nanowires. It is difficult to observe Cu nanowires in the case of no preformed Cu seeds present (Figure 3b) at identical conditions, thereby excluding the possibility of self-seeded Cu nanowire growth. This phenomenon suggests that five-twinned Cu nanocrystals have relatively few OLA molecules bound on the {111} facets of seeds, making them serve as effective seeds to foster the growth of Cu nanowires. The nanowires grow along ⟨110⟩ direction, which

dx.doi.org/10.1021/la4036198 | *Langmuir* 2014, 30, 602−610

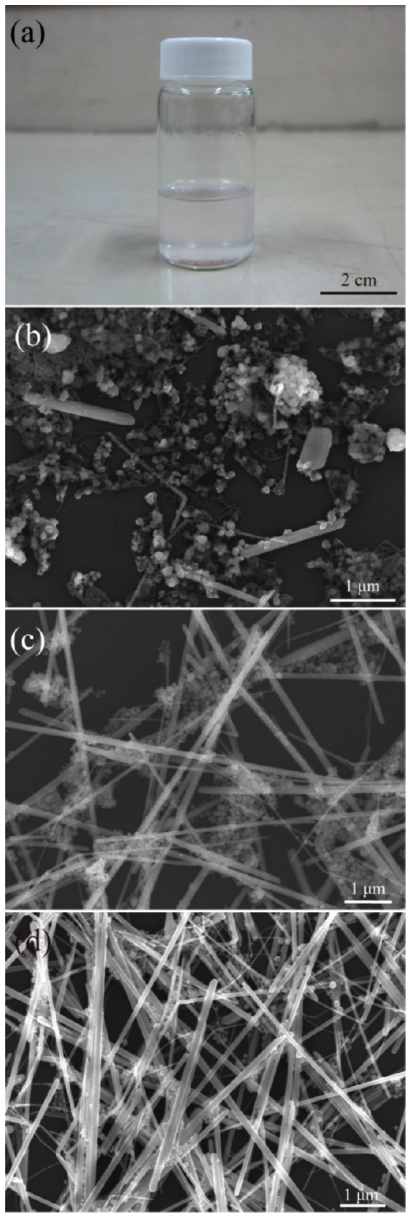

Figure 7. (a) Photoimage of CuCl/ODE mixture after 61 h heating; the mixture did not change significantly after the reaction. SEM images of Cu nanostructures synthesized at (b) 0.12 mL OLA + 4.88 mL ODE, (c) 0.36 mL OLA + 4.64 mL ODE, and (d) 1 mL OLA + 4 mL ODE.

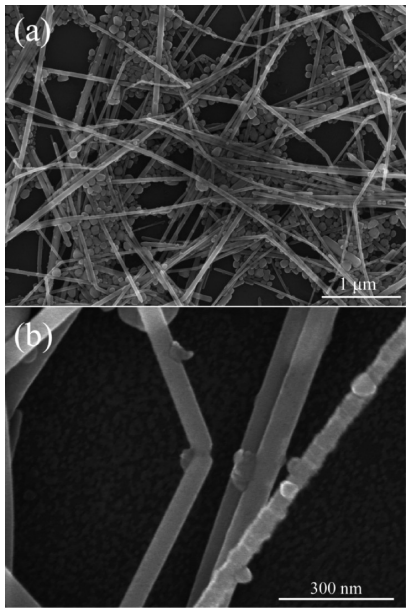

Figure 8. (a) Cu nanowires produced by using preformed five-twinned Cu nanocrystals as seeds at 170 °C for 12 h. (b) SEM image of a V shape Cu nanowire.

may be attributed to preferential adsorption of OLA on the {100} facets. Third, V shape nanowires can occasionally be observed under SEM analysis (Figure 8b), probably because the two adjacent five-twinned seeds fuse together because of relatively poor capped {111} facets and further grow into nanowires on their own. According to the above experimental results, we can speculate that the OLA preferentially adsorbs on the {100} facets of growing crystals. Compared with a relatively new self-seeded method for Cu nanowires driven by screw dislocations published in 2012,[51] we did not observe the polycrystalline seed on the Cu nanowire tip and the distinct dislocation line in the middle of nanowires. In addition, Cu nanowires driven by screw dislocations show single crystalline nature, not five-twinned structure. Basically, the growth mechanism of copper nanowires in our approach is different with the dislocation-driven case. The schematic of the proposed growth mechanism is shown in Figure 9.

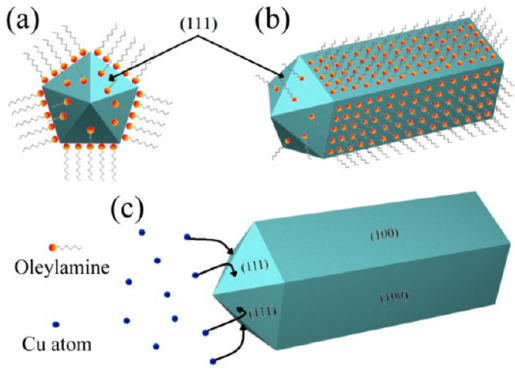

Figure 9. Proposed growth mechanism for Cu nanowires grown via a seed-mediated method. (a) Five-twinned seeds generated by homogeneous nucleation. (b) OLA tends to adsorb on {100} facets because of more open sites. (c) Cu atoms deposit and recrystallize on the relatively poor capped {111} facets, promoting the anisotropic growth of Cu crystals.

The electrical resistivity of a single Cu nanowire was measured at room temperature by using a four-probe technique. Figure 10b shows the $I-V$ characteristic curve obtained from a four-point connected Cu nanowire having 75-nm diameter and 18-μm length. The nanowire device is shown in Figure 10a. A linear $I-V$ curve was obtained, which indicates ohmic properties at room temperature. The contact resistivity of the nanowire can be calculated with the following equation:

$$\rho = (R \times A)/(L)$$

where R is the measured resistance, and ρ denotes the resistivity of the material. Here, A and L are the nanowire cross-sectional area and length, respectively. The calculated resistivity (ρ) of the nanowire is 41.25 nΩ-m, which is approximately 2.45 times greater than that of bulk copper (16.78 nΩ-m) but is of

dx.doi.org/10.1021/la4036198 | Langmuir 2014, 30, 602−610

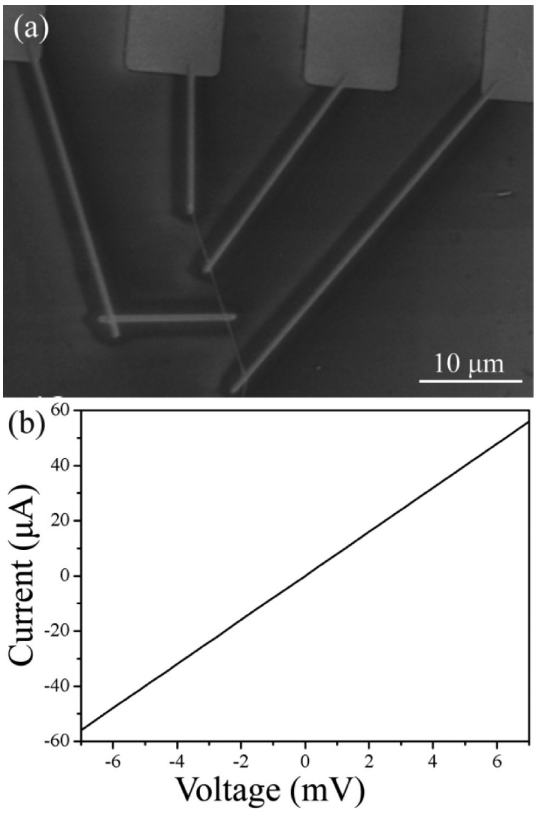

Figure 10. (a) SEM image of the Cu nanowire with contact to four electrodes by the deposited platinum. (b) Electrical transport measurement on a single Cu nanowire obtained from four-probe measurements.

the same order of magnitude as the value of bulk copper (16.78 nΩ-m).

Moreover, the SERS substrates made of Cu nanowires were analyzed by measuring the SERS spectra of Cu nanowires on Si substrate using 4-MBA as the model molecule. According to our SEM Analysis, the Cu nanowires almost cover the entire substrates (Figure 11a). The measured SERS spectra of Cu nanowires on the Si substrate and normal Raman spectra of solid 4-MBA are shown in Figure 11b and Figure S1, respectively. Both spectra have typical signals at approximately 1080 and 1590 cm^{-1} owing to aromatic ring vibrations. The characteristic bands of 4-MBA include those at 1080 and 1590 cm^{-1} owing to aromatic ring vibrations and other less intense modes, at approximately 1150 and 1180 cm^{-1} caused by C−H deformation, and at ∼1400 cm^{-1} caused by the presence of some COO groups from deprotonation of 4-MBA molecules on the Cu nanowire SERS substrate.[52]

In general, the enhancement factor (EF) for SERS is calculated using the following equation:

$$EF = [I_{SERS}] \times [M_{bulk}]/[I_{bulk}] \times [M_{SERS}]$$

where I_{SERS} and I_{bulk} are the intensity of the same Raman band for the SERS and normal Raman spectra. M_{bulk} is the number of molecules probed in a bulk sample which is determined on the basis of the illuminated volume (about 1.57 μm^3) of our laser and the solid 4-MBA for the bulk value (Figure S1). M_{SERS} is the number of molecules bound to Cu nanowires on the SERS substrate which is calculated by the monolayer-absorbed mode (three 4-MBA molecules occupy 1 nm^2).[52−54] The intensity of the ν(CC) ring-breathing mode (1080 cm^{-1}) was chosen to

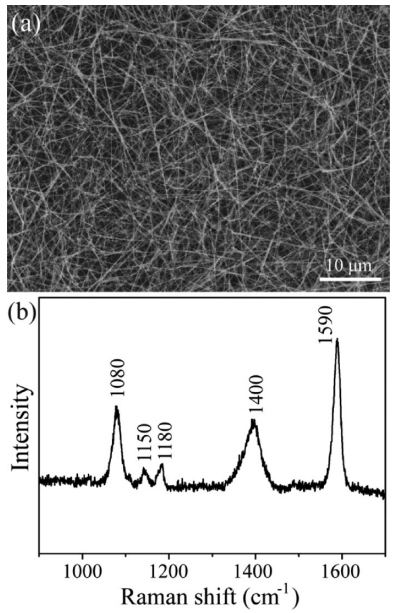

Figure 11. (a) SEM image of SERS substrate made of Cu nanowires. (b) SERS spectra of 4-MBA (2.5 mM) on SERS substrates.

calculate the enhancement factor (EF) of the SERS substrates made of Cu nanowires. The EF value for 4-MBA on Cu nanowires is about 1.1×10^4 compared to the normal Raman spectrum of solid 4-MBA. In addition, the EF value is sensitive to the exact SERS conditions (including analyte and the shape, size, size distribution, surface state, and the nature of the metal nanostructures).[55]

CONCLUSION

In summary, we achieved some progress in the field of synthesis and applications of Cu nanowires. First, the present work provides a comprehensive mechanistic study on the self-seeded growth of Cu nanowires as well as the detailed structure and electrical characterization of pentagonal Cu nanowires synthesized from five-twinned seeds which has been relatively neglected in the past. The growth process was monitored with an electron microscope and by measuring UV−visible spectra. During the nanowire growth process, five-twinned seeds were obtained at the initial stage of reaction. Thereafter, the nanorods appeared as a result of the combination of internal confinement provided by five-twinned structure, Cu atoms offered by the Ostwald ripening process, and the reduction reactions of the CuCl−OLA complex. Second, some indirect evidence for the role of the OLA bound to the {100} planes of the Cu nanowires in the growth process is also presented. OLA effectively stabilizes the newly formed {100} surfaces rather than the {111} surfaces, leading to the formation of five-twinned Cu nanowires. Further, a single Cu nanowire has a very low resistivity of 41.25 nΩ-m, which is of the same order of magnitude as the value of bulk Cu. Finally, for the first time, the active SERS substrate made of Cu nanowires is shown to enhance the Raman signals with an EF value of 1.1×10^4 by using 4-MBA as the probe molecule. These results show that five-twinned Cu nanowires have many properties suitable for a wide range of applications, such as electrical interconnections, transparent conducting electrodes, medical diagnosis, and biological analysis.

dx.doi.org/10.1021/la4036198 | Langmuir 2014, 30, 602−610

■ ASSOCIATED CONTENT

Supporting Information

Raman spectra of solid 4-MBA. This material is available free of charge via the Internet at http://pubs.acs.org.

■ AUTHOR INFORMATION

Corresponding Author

*Tel: + 886-3-572-3661. Fax: + 886-3-571-5408. E-mail: hytuan@che.nthu.edu.tw.

Notes

The authors declare no competing financial interest.

■ ACKNOWLEDGMENTS

The authors acknowledge the financial support by the National Science Council of Taiwan (NSC 102-2221-E-007-023-MY3, NSC 102-2221-E-007-090-MY2, and NSC 101-2623-E-007-013-IT), the Minitry of Economic Affairs, Taiwan (101-EC-17-A-09-S1-198), and National Tsing Hua University (102N2051E1, 102N2061E1) and the assistance from Center for Energy and Environmental Research, National Tsing-Hua University.

■ REFERENCES

(1) Yong, C.; Zhang, B. C.; Seet, C. S.; See, A.; Chan, L.; Sudijono, J.; Liew, S. L.; Tung, C. H.; Zeng, H. C. Cool copper template for the formation of oriented nanocrystalline α-tantalum. *J. Phys. Chem. B* **2002**, *106*, 12366−12368.

(2) Monson, C. F.; Woolley, A. T. DNA-templated construction of copper nanowires. *Nano Lett.* **2003**, *3*, 359−363.

(3) Tran, T. T.; Lu, X. Synergistic effect of Ag and Pd ions on shape-selective growth of polyhedral Au nanocrystals with high-index facets. *J. Phys. Chem. C* **2011**, *115*, 3638−3645.

(4) Wen, X. G.; Xie, Y. T.; Choi, C. L.; Wan, K. C.; Li, X. Y.; Yang, S. H. Copper-based nanowire materials: Templated syntheses, characterizations, and applications. *Langmuir* **2005**, *21*, 4729−4737.

(5) Pang, Y. T.; Meng, G. W.; Zhang, Y.; Fang, Q.; Zhang, L. D. Copper nanowire arrays for infrared polarizer. *Appl. Phys. A: Mater. Sci. Process.* **2003**, *76*, 533−536.

(6) Rathmell, A. R.; Bergin, S. M.; Hua, Y. L.; Li, Z. Y.; Wiley, B. J. The growth mechanism of copper nanowires and their properties in flexible, transparent conducting films. *Adv. Mater.* **2010**, *22*, 3558−3563.

(7) Wu, J.; Zang, J.; Rathmell, A. R.; Zhao, X.; Wiley, B. J. Reversible sliding in networks of nanowires. *Nano Lett.* **2013**, *13*, 2381−2386.

(8) Rathmell, A. R.; Nguyen, M.; Chi, M.; Wiley, B. J. Synthesis of oxidation-resistant cupronickel nanowires for transparent conducting nanowire networks. *Nano Lett.* **2012**, *12*, 3913−3199.

(9) Rathmell, A. R.; Wiley, B. J. The synthesis and coating of long, thin copper nanowires to make flexible, transparent conducting films on plastic substrates. *Adv. Mater.* **2011**, *23*, 4798−4803.

(10) Zhang, D.; Wang, R.; Wen, M.; Weng, D.; Cui, X.; Sun, J.; Li, H.; Lu, Y. Synthesis of ultralong copper nanowires for high-performance transparent electrodes. *J. Am. Chem. Soc.* **2012**, *134*, 14283−14286.

(11) Lu, X.; Yavuz, M. S.; Tuan, H.-Y.; Korgel, B. A.; Xia, Y. Ultrathin gold nanowires can be obtained by reducing polymeric strands of oleylamine−AuCl complexes formed via aurophilic interaction. *J. Am. Chem. Soc.* **2008**, *130*, 8900−8901.

(12) Xu, J.; Wang, Y.; Qi, X.; Liu, C.; He, J.; Zhang, H.; Chen, H. Preservation of lattice orientation in coalescing imperfectly aligned gold nanowires by a zipper mechanism. *Angew. Chem., Int. Ed.* **2013**, *52*, 6019−6023.

(13) He, J.; Wang, Y.; Feng, Y.; Qi, X.; Zeng, Z.; Liu, Q.; Teo, W. S.; Gan, C. L.; Zhang, H.; Chen, H. Forest of gold nanowires: A new type of nanocrystal growth. *ACS Nano* **2013**, *7*, 2733−2740.

(14) Velázquez-Salazar, J. J.; Esparza, R.; Mejía-Rosales, S. J.; Estrada-Salas, R.; Ponce, A.; Deepak, F. L.; Castro-Guerrero, C.; José-Yacamán, M. Experimental evidence of icosahedral and decahedral packing in one-dimensional nanostructures. *ACS Nano* **2011**, *5*, 6272−6278.

(15) Sun, Y. Controlled synthesis of colloidal silver nanoparticles in organic solutions: Empirical rules for nucleation engineering. *Chem. Soc. Rev.* **2013**, *42*, 2497−2511.

(16) Liu, Z. P.; Yang, Y.; Liang, J. B.; Hu, Z. K.; Li, S.; Peng, S.; Qian, Y. T. Synthesis of copper nanowires via a complex-surfactant-assisted hydrothermal reduction process. *J. Phys. Chem. B* **2003**, *107*, 12658−12661.

(17) Chang, Y.; Lye, M. L.; Zeng, H. C. Large-scale synthesis of high-quality ultralong copper nanowires. *Langmuir* **2005**, *21*, 3746−3748.

(18) Shi, Y.; Li, H.; Chen, L. Q.; Huang, X. J. Obtaining ultra-long copper nanowires via a hydrothermal process. *Sci. Technol. Adv. Mat.* **2005**, *6*, 761−765.

(19) Ye, E. Y.; Zhang, S. Y.; Liu, S. H.; Han, M. Y. Disproportionation for growing copper nanowires and their controlled self-assembly facilitated by ligand exchange. *Chem.—Eur. J.* **2011**, *17*, 3074−3077.

(20) Cho, Y. S.; Huh, Y. D. Synthesis of ultralong copper nanowires by reduction of copper-amine complexes. *Mater. Lett.* **2009**, *63*, 227−229.

(21) Mohl, M.; Pusztai, P.; Kukovecz, A.; Konya, Z. Low-temperature large-scale synthesis and electrical testing of ultralong copper nanowires. *Langmuir* **2010**, *26*, 16496−16502.

(22) Sun, Y. G.; Yin, Y. D.; Mayers, B. T.; Herricks, T.; Xia, Y. N. Uniform silver nanowires synthesis by reducing $AgNO_3$ with ethylene glycol in the presence of seeds and poly(vinyl pyrrolidone). *Chem. Mater.* **2002**, *14*, 4736−4745.

(23) Murphy, C. J.; Jana, N. R. Controlling the aspect ratio of inorganic nanorods and nanowires. *Adv. Mater.* **2002**, *14*, 80−82.

(24) Jana, N. R.; Gearheart, L.; Murphy, C. J. Wet chemical synthesis of silver nanorods and nanowires of controllable aspect ratio. *Chem. Commun.* **2001**, 617−618.

(25) Gole, A.; Murphy, C. J. Seed-mediated synthesis of gold nanorods: Role of the size and nature of the seed. *Chem. Mater.* **2004**, *16*, 3633−3640.

(26) Zhu, L.; Shen, X.; Zeng, Z.; Wang, H.; Zhang, H.; Chen, H. Induced coiling action: Exploring the intrinsic defects in five-fold twinned silver nanowires. *ACS Nano* **2012**, *6*, 6033−6039.

(27) Mayoral, A.; Allard, L. F.; Ferrer, D.; Esparza, R.; Jose-Yacaman, M. On the behavior of Ag nanowires under high temperature: In situ characterization by aberration-corrected STEM. *J. Mater. Chem.* **2011**, *21*, 893−898.

(28) Sun, Y.; Wang, Y. Monitoring of galvanic replacement reaction between silver nanowires and $HAuCl_4$ by in situ transmission X-ray microscopy. *Nano Lett* **2011**, *11*, 4386−4392.

(29) Xia, Y. N.; Xiong, Y. J.; Lim, B.; Skrabalak, S. E. Shape-controlled synthesis of metal nanocrystals: Simple chemistry meets complex physics? *Angew. Chem., Int. Ed.* **2009**, *48*, 60−103.

(30) Elechiguerra, J. L.; Reyes-Gasga, J.; Yacaman, M. J. The role of twinning in shape evolution of anisotropic noble metal nanostructures. *J. Mater. Chem.* **2006**, *16*, 3906−3919.

(31) Wang, J. H.; Yang, T. H.; Wu, W. W.; Chen, L. J.; Chen, C. H.; Chu, C. J. Synthesis and growth mechanism of pentagonal Cu nanobats with field emission characteristics. *Nanotechnology* **2006**, *17*, 719−722.

(32) Nepijko, S. A.; Ievlev, D. N.; Schulze, W.; Urban, J.; Ertl, G. Growth of rodlike silver nanoparticles by vapor deposition of small clusters. *ChemPhysChem* **2000**, *1*, 140−142.

(33) Bogels, G.; Meekes, H.; Bennema, P.; Bollen, D. Growth mechanism of vapor-grown silver crystals: Relation between twin formation and morphology. *J. Phys. Chem. B* **1999**, *103*, 7577−7583.

(34) Elechiguerra, J. L.; Larios-Lopez, L.; Liu, C.; Garcia-Gutierrez, D.; Camacho-Bragado, A.; Jose-Yacaman, M. Corrosion at the nanoscale: The case of silver nanowires and nanoparticles. *Chem. Mater.* **2005**, *17*, 6042−6052.

(35) Sun, Y. G.; Mayers, B.; Herricks, T.; Xia, Y. N. Polyol synthesis of uniform silver nanowires: A plausible growth mechanism and the supporting evidence. *Nano Lett* **2003**, *3*, 955−960.
(36) Johnson, C. J.; Dujardin, E.; Davis, S. A.; Murphy, C. J.; Mann, S. Growth and form of gold nanorods prepared by seed-mediated, surfactant-directed synthesis. *J. Mater. Chem.* **2002**, *12*, 1765−1770.
(37) Chen, H. Y.; Gao, Y.; Zhang, H. R.; Liu, L. B.; Yu, H. C.; Tian, H. F.; Xie, S. S.; Li, J. Q. Transmission-electron-microscopy study on five-fold twinned silver nanorods. *J. Phys. Chem. B* **2004**, *108*, 12038−12043.
(38) Wiley, B.; Sun, Y. G.; Mayers, B.; Xia, Y. N. Shape-controlled synthesis of metal nanostructures: The case of silver. *Chem.—Eur. J.* **2005**, *11*, 454−463.
(39) Mourdikoudis, S.; Liz-Marzán, L. M. Oleylamine in nanoparticle synthesis. *Chem. Mater.* **2013**, *25*, 1465−1476.
(40) Hutter, E.; Fendler, J. H. Exploitation of localized surface plasmon resonance. *Adv. Mater.* **2004**, *16*, 1685−1706.
(41) Zhang, L.; Jing, H.; Boisvert, G.; He, J. Z.; Wang, H. Geometry control and optical tunability of metal−cuprous oxide core−shell nanoparticles. *ACS Nano* **2012**, *6*, 3514−3527.
(42) Zhang, L.; Blom, D. A.; Wang, H. Au−Cu_2O core−shell nanoparticles: A hybrid metal−semiconductor heteronanostructure with geometrically tunable optical properties. *Chem. Mater.* **2011**, *23*, 4587−4598.
(43) Ni, C. Y.; Hassan, P. A.; Kaler, E. W. Structural characteristics and growth of pentagonal silver nanorods prepared by a surfactant method. *Langmuir* **2005**, *21*, 3334−3337.
(44) Lisiecki, I.; Filankembo, A.; Sack-Kongehl, H.; Weiss, K.; Pileni, M. P.; Urban, J. Structural investigations of copper nanorods by high-resolution TEM. *Phys. Rev. B* **2000**, *61*, 4968−4974.
(45) Kim, C.; Gu, W. H.; Briceno, M.; Robertson, I. M.; Choi, H.; Kim, K. Copper nanowires with a five-twinned structure grown by chemical vapor deposition. *Adv. Mater.* **2008**, *20*, 1859−1863.
(46) Reyes-Gasga, J.; Elechiguerra, J. L.; Liu, C.; Camacho-Bragado, A.; Montejano-Carrizales, J. M.; Yacaman, M. J. On the structure of nanorods and nanowires with pentagonal cross-sections. *J. Cryst. Growth* **2006**, *286*, 162−172.
(47) Elechiguerra, J. L.; Reyes-Gasga, J.; Yacaman, M. J. The role of twinning in shape evolution of anisotropic noble metal nanostructures. *J. Mater. Chem.* **2006**, *16*, 3906−3919.
(48) Ming, N. B.; Sunagawa, I. Twin lamellae as possible self-perpetuating step sources. *J. Cryst. Growth* **1988**, *87*, 13−17.
(49) Yin, Y.; Alivisatos, A. P. Colloidal nanocrystal synthesis and the organic−inorganic interface. *Nature* **2005**, *437*, 664−670.
(50) Quan, Z.; Yang, P.; Li, C.; Yang, J.; Yang, D.; Jin, Y.; Lian, H.; Li, H.; Lin, J. Shape and phase-controlled synthesis of $KMgF_3$ colloidal nanocrystals via microwave irradiation. *J. Phys. Chem. C* **2009**, *113*, 4018−4025.
(51) Meng, F.; Jin, S. The solution growth of copper nanowires and nanotubes is driven by screw dislocations. *Nano Lett.* **2012**, *12*, 234−239.
(52) Hunyadi, S. E.; Murphy, C. J. Bimetallic silver-gold nanowires: Fabrication and use in surface-enhanced Raman scattering. *J. Mater. Chem.* **2006**, *16*, 3929−3935.
(53) He, Y.; Su, S.; Xu, T. T.; Zhong, Y. L.; Zapien, J. A.; Li, J.; Fan, C. H.; Lee, S. T. Silicon nanowires-based highly-efficient SERS-active platform for ultrasensitive DNA detection. *Nano Today* **2011**, *6*, 122−130.
(54) He, D.; Hu, B.; Yao, Q. F.; Wang, K.; Yu, S. H. Large-scale synthesis of flexible free-standing SERS substrates with high sensitivity: Electrospun PVA nanofibers embedded with controlled alignment of silver nanoparticles. *ACS Nano* **2009**, *3*, 3993−4002.
(55) Le Ru, E. C.; Blackie, E.; Meyer, M.; Etchegoin, P. G. Surface enhanced Raman scattering enhancement factors: A comprehensive study. *J. Phys. Chem. C* **2007**, *111*, 13794−13803.